2022 IEEE/RSJ International Conference on Intelligent Robots and Systems (IROS)
October 23-27, 2022, Kyoto, Japan

Development and Experimental Evaluation of a Novel Portable Haptic Robotic Exoskeleton Glove System for Patients with Brachial Plexus Injuries

Wenda Xu[1], Yunfei Guo[2], Cesar Bravo[3] and Pinhas Ben-Tzvi[4]

2022 IEEE/RSJ International Conference on Intelligent Robots and Systems (IROS) | 978-1-6654-7927-1/22/$31.00 ©2022 IEEE | DOI: 10.1109/IROS47612.2022.9981468

***Abstract*— This paper presents the development and experimental evaluation of a portable haptic exoskeleton glove system designed for people who suffer from brachial plexus injuries to restore their lost grasping functionality. The proposed glove system involves force perception, linkage-driven finger mechanism, and personalized voice control to achieve various grasping functionality requirements. The fully integrated system provides our wearable device with lightweight, portable, and comfortable characterization for grasping objects used in daily activities. Rigid articulated linkages powered by Series Elastic Actuators (SEAs) with slip detection on the fingertips provide stable and robust grasp for multiple objects. The passive abduction-adduction motion of each finger is also considered to provide better grasping flexibility for the user. The continuous voice control with bio-authentication also provides a hands-free user interface. The experiments with different objects verify the functionalities and capabilities of the proposed exoskeleton glove system in grasping objects with various shapes and weights used in activities of daily living (ADLs).**

***Index Terms*— Rehabilitation Robotics, Exoskeleton Glove, Series Elastic Actuator, Wearable Robotics**

I. INTRODUCTION

Brachial plexus injury (BPI) is usually caused by motor vehicle accidents and extreme sporting accidents. Patients with such injuries suffer from lack of muscle control and sensation in the arm, hand and wrist. Previous studies have found that surgical options can restore shoulder and arm function, but much less so in returning sensation and mobility to the hand and wrist [1].

A promising approach to help patients perform ADLs is to use exoskeleton devices.A number of hand rehabilitation designs in previous research can be categorized into three major categories: Soft robotic gloves [2], [3], cable-driven gloves [4], [5], and linkage-driven gloves [6], [7]. However, these designs suffer from several disadvantages, such as bulky shape, heavy weight and the need for multiple actuators. The glove wearability, comfortability, and portability are limited by their mechanism, actuators or controllers.

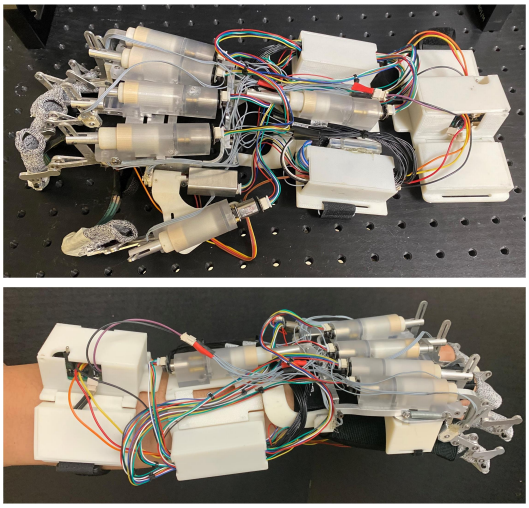

Fig. 1. Different views of the robotic glove exoskeleton used in this research.

Given the shortcomings of previous wearable devices, we developed a new exoskeleton glove system that is portable and multi-functional for various grasping functions. Fig. 1 shows different views of the entire glove system. The whole glove is controlled by customized voice commands and driven by SEAs [8]. The spring elements in the SEA provide accurate force measurement and smooth force control. The optimized linkage system couples the motion of the metacarpophalangeal (MCP), proximal interphalangeal (PIP), and distal interphalangeal (DIP) joints into one degree of freedom fastened alongside the finger (Fig. 2) [9]. Besides the basic bending mechanism of each finger, passive abduction-adduction degrees of freedom have been implemented. To achieve better grasping performance, the coupled motion of the wrist and the hand have been also taken into account. Furthermore, the micro-controller and battery are integrated on the wrist for better portability.

The main contributions presented in this paper include the development of the complete robotic glove system based on previous research work [9], [10], and the presented grasping experiments conducted with various objects and tasks. The integration of finger mechanisms, actuators, microcontrollers and voice activation make our proposed glove

Research reported in this publication was supported by the Eunice Kennedy Shriver National Institute of Child Health & Human Development of the National Institutes of Health under Award Number R21HD095027. The content is solely the responsibility of the authors and does not necessarily represent the official views of the National Institutes of Health.
(Corresponding author: Pinhas Ben-Tzvi)

[1]Wenda Xu is with the Department of Mechanical Engineering, Virginia Tech, Blacksburg, VA, 24061 USA (e-mail: wenda@vt.edu).

[2]Yunfei Guo is with the Department of Electrical and Computer Engineering, Virginia Tech, Blacksburg, VA 24061 USA (e-mail: yunfei96@vt.edu).

[3]Cesar Bravo is with the Carilion Clinic Institute of Orthopaedics and Neurosciences, Virginia Tech Carilion School of Medicine, Roanoke, VA 24016 USA (e-mail: cjbravo@carilionclinic.org).

[4]Pinhas Ben-Tzvi is with the Departments of Mechanical Engineering and Electrical and Computer Engineering, Virginia Tech, Blacksburg, VA, 24061 USA (e-mail: bentzvi@vt.edu).

system portable, lightweight and more capable than before. It also provides portability for patients' normal wear and daily use. Furthermore, with the combination of hand rehabilitation learning system, the developed system provides patients with grasp adjustments capability based on the finger motions and contact forces for grasping different objects.

The rest of the paper is organized as follows. In section II, the specifications of the system are described. In section III, the development of the entire glove system is introduced including two types of SEAs, linkages, and the full glove. Section IV introduces the electronics design, the control principle, and the integration of the micro-controller for the glove system. Section V demonstrates the controller performance, the experiments performed with the glove, and a comparison with other devices. Lastly, section VI concludes the paper.

II. SYSTEM OVERVIEW

The goal of the proposed glove system is to help restore the grasping functionality for patients with BPIs to perform ADLs. Based on previous research [11], we simplified the 33 static and stable grasp types [12] into 5 daily used grasp types, which include Cylinder, Sphere, Tripod, Tip, and Lateral grasps. The current system can provide up to $10N$ of contact force on each finger and grasp objects with diameters from $24mm$ to $82mm$. Since a normal grasp consists of coupled motion of the hand and the wrist [13], our system also supports 25° in wrist extension and 15° in wrist flexion. The total weight of the whole system is 759 g.

The glove system is activated and controlled by voice commands. The voice commands indicate the prospective grasp type directly to the system. The SEAs work as the actuation units as well as the force sensors. The Force Sensitive Resistor (FSR) sensors only provide contact detection and slip detection for the force adjustment on each finger due to their low accuracy.

III. MECHANICAL DESIGN

The mechanism of the proposed glove system consists of SEAs (including five Linear SEAs [10] and one Rotary SEA) as the actuation units, which generate and measure force or torque for each finger, and rigid linkages [9] as the output elements, which mimic actual human fingers to execute various grasping motions. The perspective view in Fig. 2 shows the components of the index finger SEA and linkage. The screw nut is constrained by the inner surface of the housing to provide linear motion. There are two wave disk springs placed inside the screw nut. The back spring is used to provide elastic connection between the output shaft and the screw nut, and the front spring works as a buffer for the force absorption when restoring the hand motion after a grasp. The Linear SEA (LSEA) and finger mechanism are connected by a variation on a crank slider mechanism, and thus the linear motion is transformed to rotation.

The exoskeleton finger linkages are attached to the side of each finger to drive the patient's hand. Based on previous research [9], the length and shape of each finger link are designed and optimized by finding the conditional minimum of the human finger motion imitating the grasp of small objects. The passive abduction-adduction function is also considered while performing the grasp by adding a revolute joint under each LSEA and using the side installed spring to hold the initial neutral position.

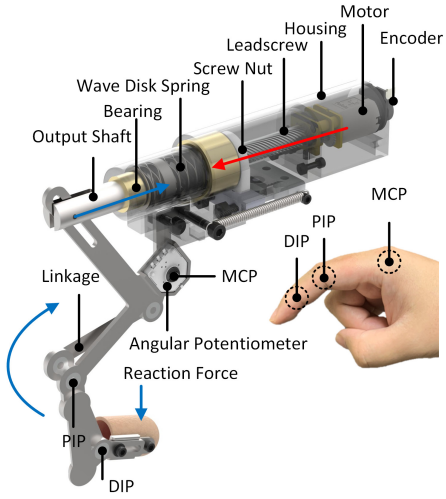

Fig. 2. Perspective View of the index linkage. The screw nut guided by the leadscrew connects the output shaft. The compressed wave disk spring between the output shaft and screw nut measures the force by its deformation when the fingertip makes contact with an object. The red arrow shows the force generation flow and the blue arrow shows the force measurement flow.

The proposed LSEA and finger linkage mechanism combination can provide stable, continuous as well as force control for grasping. The motor-generated torque is transmitted to the output force of a LSEA through a gearbox, leadscrew-driven motion, and wave disk spring. Based on the regular leadscrew load-lifting equation, the output force F_o at the SEA output shaft, related to the input stall torque T_m from the motor, can be calculated according to:

$$F_o = \frac{2T_m i}{d_m}\left(\frac{1-\mu\sec\alpha\tan\lambda}{\mu\sec\alpha+\tan\lambda}\right)\eta_s\eta_g\eta_m \qquad (1)$$

where d_m is the pitch diameter; λ is the lead angle; α is the thread angle; μ is the friction coefficient; i is the reduction rate; η_s is the efficiency of the leadscrew; η_g is the transmission efficiency; and η_m is the efficiency of the motor combination. The efficiency of the leadscrew and the efficiency of the motor combination are provided in product specifications sheet. The transmission efficiency is defined as the ratio of the output force and the input force.

The above equations specify the largest force that can be generated from the LSEA when the spring is rigid or under no load. However, due to the soft connection between the output shaft and screw nut, the actual output force of the LSEA equals to the compression force generated by the wave disk spring for normal use. Assuming that all frictions are small enough to be neglected and sensors are accurate enough without noise, the actual output force F_{ao} of the LSEA can be calculated according to:

$$F_{ao} = [\Delta d - h\cdot(tan(\theta_i+\Delta\theta) - tan(\theta_i))]\cdot k \qquad (2)$$

where $\Delta d = \frac{\Delta x \cdot l}{CPR \cdot i}$ is the screw nut moving distance from the initial position; Δx is the reading difference of the encoder compared with the initial position; l is the lead of the leadscrew. CPR refers to the count per revolution of the encoder; h is the height of the output shaft compared with the center of rotation; $\Delta\theta$ refers to the rotation angle; and θ_i is the initial angle. Both θ and θ_i can be obtained from the angular potentiometer. k is the spring constant.

Assuming that the action force F_a on the finger tip is perpendicular to the last linkage, which equals to the reaction force F_r generated by the object, the action force can be calculated by $F_a = F_r = \frac{F_{ao} \cdot h}{L}$, where L is the distance between the pivot to the action force.

As for the Rotary SEA (RSEA), it is also required to provide two major functionalities, which include force generation and force measurement. Fig. 3 shows the section view of the RSEA. The inner shaft is connected to the motor directly. One leg of the torsion spring is fixed in the groove of the inner shaft while the other is fixed in the groove of the thumb thenar, and thus the thumb thenar is elastically connected with the inner shaft. When the user performs a grasp, the difference of the rotation angle between the inner shaft and the thumb thenar is used to calculate the torque which is applied to the thumb thenar as $\tau = \kappa\Delta\theta$, where τ is the generated torque; κ is the torsion constant and $\Delta\theta$ is the angle difference from the inner shaft and thumb thenar read by the angular potentiometer. To avoid the effect of gravity on the mechanism, a rigid block is added to consistently hold the initial position.

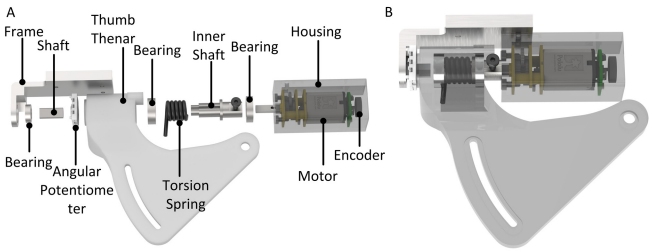

Fig. 3. Design of RSEA for thumb thenar: (A) Exploded view of the RSEA, (B) Perspective view of the RSEA.

To achieve better performance while performing daily activities, each finger should be powerful enough to provide suitable contact force. We selected 9 objects for daily use (shown in Table I), which were subjected to 5 grasp types, to estimate the reaction force on each finger based on their shape and weight. Considering the mechanical advantage of the finger linkage and the weight of selected objects, the LSEA is designed to measure up to 10N. To satisfy the design requirements and maintain the small size of the transmission system, the wave disk spring ($k = 4.15$N·mm, $load = 30$N), the dual shaft gear motors ($i = 380:1$, $T_m = 490$ N·mm, $n_m = 32300$RPM) and the leadscrew ($l = 20$mm, $d_m = 5.5$mm, $\alpha = 30°$, $\mu = 0.2$, $\eta_s = 0.78$, $\lambda = 49.27°$) have been selected.

TABLE I
GRASPED OBJECTS

Object	Weight (g)	Type	Object	Weight (g)	Type
Small Bottle	400	Cylinder	Tape	33	Tip
Large Bottle	1000	Cylinder	Tennis Ball	69	Sphere
Marker	15	Tripod	Apple	193	Sphere
Pen	9	Tripod	Bowl	319	Lateral
Paper Box	4	Tip			

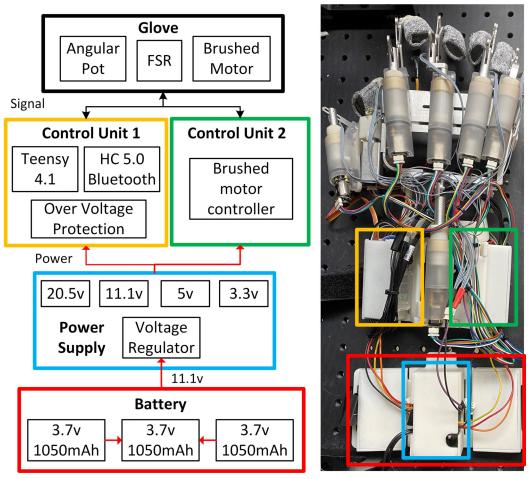

Fig. 4. Electronics design overview. Yellow: Micro-controller board. Green: Brushed motor controller board. Blue: Power conversion board. Red: 3-in-1 battery package.

IV. ELECTRONICS AND CONTROL SYSTEM DESIGN

The glove's on-board electronics consist of four parts, three separate PCBs, and a lithium-ion battery pack, as shown in Fig. 4. Three separate PCBs have two control units that process the signal from sensors and control the motor. One of the PCBs is dedicated to power conversion to provide various voltages to the system. The lithium-ion battery pack contains three batteries (3.7V 1050 mAh) in series.

The exoskeleton control system can be divided into a high-level controller running on a computer and a low-level controller running on the onboard micro-controller. The control structure is shown in Fig. 5(A).

The high-level controller consists of two parts. The first part is the voice data input from a Bluetooth Microphone, which will be sent to the configurable voice activation and speaker verification human-machine interference (CVASV HMI) [14]. The CVASV HMI supports customized activation keywords and can provide voice-based bio-authentication while converting speech to text. The CVASV HMI will be activated by the voice command gathered from the user. The type of grasps that need to be performed will be passed to the slip grasp program. The second part is the slip grasp program which starts the grasp and monitors the fingertips for slippage. If the object slips while being lifted, the system will add force to each LSEA. The force command will be sent from the computer to the micro-controller.

The low-level controller consists of three parts. First, The force command is sent to the micro-controller from the computer grasping program through Bluetooth. The force

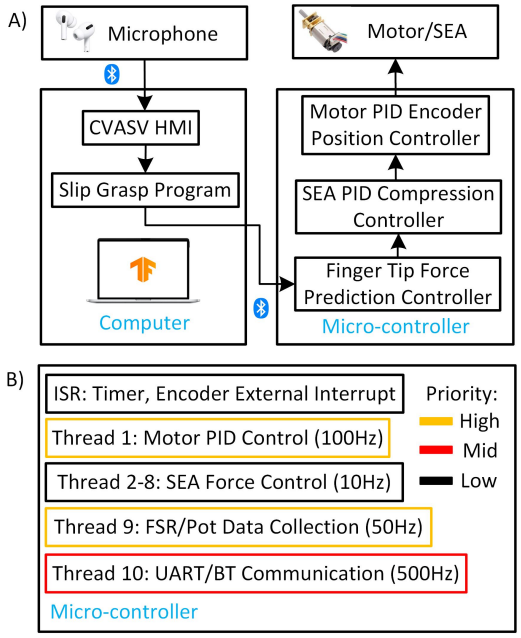

Fig. 5. (A) Control structure overview. (B) Micro-controller software architecture.

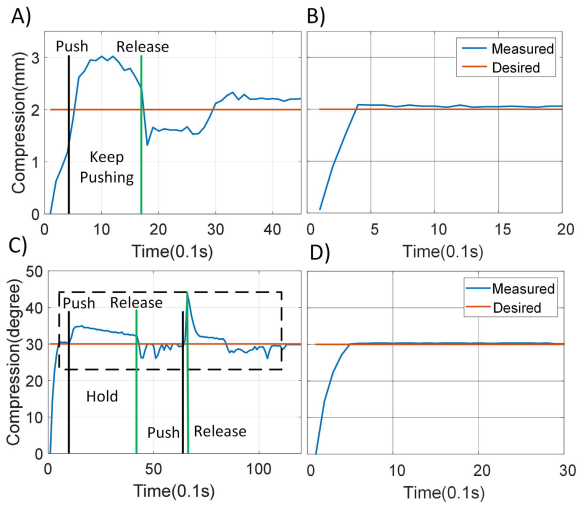

Fig. 6. (A) Impulse response of index finger linear SEA PID compression control. (B) Index finger linear SEA PID compression control. (C) Impulse response of rotary SEA PID compression control. (D) Rotary SEA PID compression control.

command indicates the amount of the output force on each fingertip. The fingertip force prediction controller converts the desired output force on the fingertips to the spring compression needed of the SEA. The forces applied on both the RSEA and the index's LSEA are converted using machine learning for better accuracy. Other SEAs are converted using traditional kinematics conversion [15]. Second, the compression will be sent to a SEA PID compression controller to control the compression. Third, the compression controller sends out a command to the PID motor distance controller to control the LSEA output shaft. The low-level controllers of all 7 SEAs used in this glove run parallel at 10Hz on a Teensy 4.1 Micro-controller using FreeRTOS to ensure minimal control latency. The software architecture of the micro-controller is shown in Fig. 5(B).

V. Experiments

A. SEA Compression Controller Performance

The experiments are aimed to test the settling time and overshoot of both the LSEA and the RSEA compression control when impulse has been introduced as an input. During the experiments, a desired compression was provided to the controller and the compression was measured using the on-board sensors. Subfigs. 6(A) and (B) show the performance of the LSEA spring compression PID controller. In Subfigure 6(A), the impulse is introduced by push and release of the last index finger linkage. The maximum overshoot during recovery is 12.4%, and the 10% settling time is 0.8 seconds. In subfigure 6(B), no impulse is introduced. The maximum overshoot is 6%, and the 10% settling time is 0.3 seconds.

Subfigures (C) and (D) in Fig. 6 show the performance of the RSEA spring compression PID controller. In subfigure (C), the impulse is introduced by push and release of the thumb thenar. The maximum overshoot during recovery is 16.7%, and the 10% settling time varies between 0.5 seconds and 0.8 seconds. In subfigure (D), no impulse is introduced. The maximum overshoot is 0.1%, and the 10% settling time is 0.4 seconds.

B. LSEA Shut Calibration with Force Sensitive Resistor

The LSEA compression measurement can be affected by the backlash of the linkage. Fig. 7(B) shows the LSEA detected compression when the motor is not moving and the linkage is wiggled by hand without compressing the spring. The LSEA can have more than 2mm of backlash.

The LSEA compression can also be affected by the error of the potentiometer. Fig. 7(A) shows the spring compression by actuating the LSEA under no load. Theoretically, the spring compression should be 0mm. However, the compression is fluctuating due to backlash and immeasurable friction force. Such fluctuation can cause inaccurate force output applied on the fingertips.

To solve the two aforementioned problems, FSRs are used to calibrate the SEAs. When contact between the fingertip and grasped object is being made, if the current spring compression is not 0mm, the current SEA compression is set to 0mm to reduce the influence of backlash from the linkage and account for sensor error. FSRs were placed on the more commonly used index and thumb fingers. The middle, ring, and little fingers' motion are coupled with the index finger. When grasping, if the index finger has contact with objects, the middle, ring, and little fingers are calibrated simultaneously to have 0mm SEA compression.

C. Hybrid Slip Detection to Assist Grasping

Slip detection on the exoskeleton glove can be achieved by monitoring the change in contact forces [16]. Either SEAs or FSRs can be used to monitor the change in contact forces, with each method having its advantages and disadvantages.

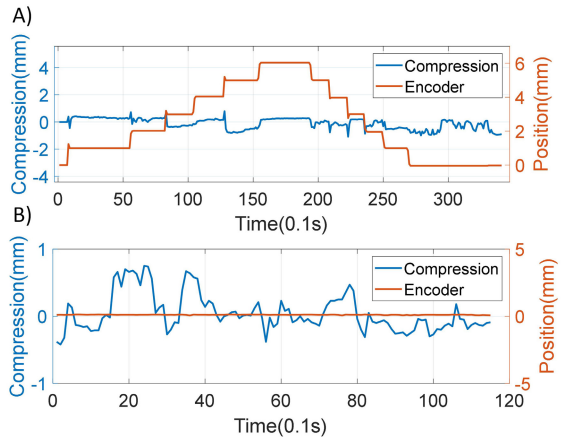

Fig. 7. Accuracy of LSEA. (A) Index finger LSEA output shaft moving with motor position PID control without load applied on SEA; (B) Wiggle index finger linkage through linkage backlash while index finger LSEA output shaft not moving.

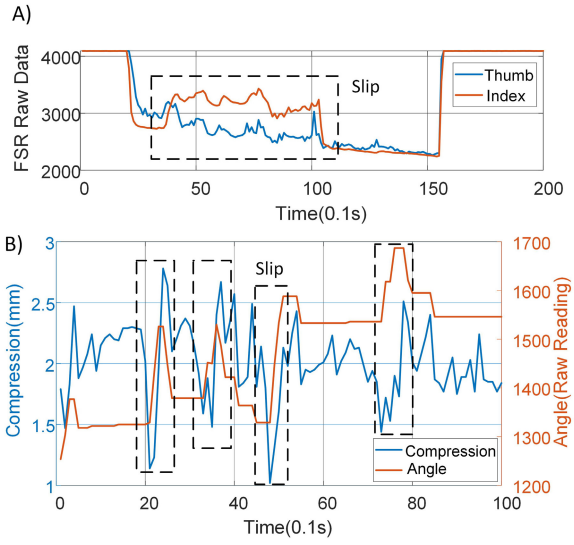

Fig. 8. SEA slip detection. (A) FSR reading while object slips (contact force is around 1N on fingertips). (B) SEA reading while object slips (contact force is around 4N on fingertips).

The error in compression on a calibrated LSEA is around 0.5mm, which means it is not sensitive when the change in contact force is less than 2.1N. The advantage of the SEA slip detection is the consistency when different amounts of force are applied due to the linear relation between force and spring compression. As shown in Fig. 8(B), when the user attempts to grasp and lift a heavy object with insufficient force, the object slips and creates a significant compression difference that can be distinguished from the sensor noise signal. However, FSRs are very sensitive to force changes. From Fig. 8(A), the FSRs can detect small force changes when 1N is applied to the fingertips. Therefore, we combined FSRs with the SEAs to detect slip.

D. Exoskeleton Glove Grasping Experiments

Experiments with 9 different objects subjected to 5 types of grasp were performed on two male participants with a healthy right hand (Fig. 9). To simulate patients with brachial plexus injuries, the participants' hands did not apply any force while grasping the objects listed in Table I.

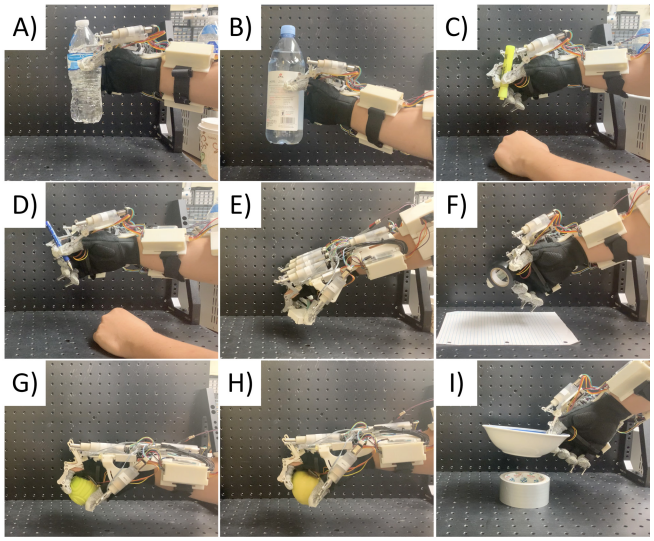

Fig. 9. Tasks performed by the participant using the proposed glove. (A) Grasping a small bottle, (B) Grasping a large bottle, (C) Grasping a marker, (D) Grasping a pen, (E) Grasping a small box, (F) Grasping a tape, (G) Grasping a tennis ball, (H) Grasping an apple, (I) Grasping a bowl.

For all 9 test objects, each participant performed 3 trials on each object. The participant was able to grasp and hold the objects with weights ranging from 4g (Fig. 9(E)) to 1000g (Fig. 9(B)). The success rate for each grasp is listed in Figure 10. It was easy to complete the cylinder grasp and sphere grasp tests due to the regular shape and size of the objects. However, to hold the larger bottle with heavy weight, our exoskeleton glove needed more time to adjust the required grasping force. This may cause the object to slip away, thereby resulting in failure of the experiments. For the tripod grasp, our glove could grasp the pen and marker with 100% success rate. The limitation of the DOFs of the proposed glove requires another person to hold the pen in position. The tip grasp is used to grasp small objects. Failure occurred when grasping the tape because the participant's hand did not reach a suitable position for grasping and the tape was squeezed out of the glove. We used the bowl to test lateral grasp and the success rate was also 100%.

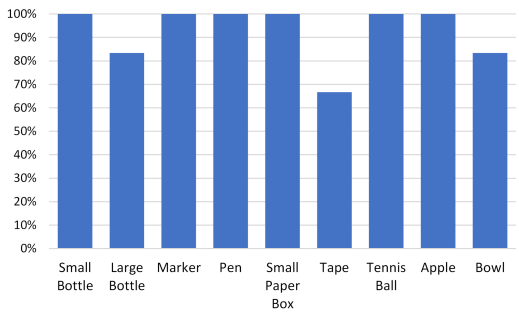

Fig. 10. Success rate of grasping each object.

TABLE II
SUMMARY OF HAND EXOSKELETON REHABILITATION SYSTEM

Device	Actuation, Transmission	Weight: glove/total	Peak Fingertip Force	Fingers
Ryu et al. [17]	hydraulics, cable	2.62 kg / 2.74 kg	12 N	3
Nycz et al. [5]	linear motor, cable	113 g / 867 g	8.7 N	4
Gloreha Lite [4]	motor, cable	80 g / 5 kg	5 N	5
Hand of Hope [6]	linear motor, linkage	700 g / -	12 N	5
Our Glove System	**SEA, linkage**	**383 g/759 g**	**10 N**	**5**

E. Comparison with Existing Exoskeleton Glove System for Rehabilitation

To better evaluate our proposed system, we compared our exoskeleton glove with four other devices as shown in Table II. It is worth mentioning that the measurements of peak fingertip force vary from device to device. We used their posted maximum pinch force or measured fingertip force to compare. Most of the glove devices on their own are lightweight, but need heavy actuators and/or are tethered to a workstation. Only a few devices are designed to actuate all five fingers. Gloves that are not able to actuate all fingers reduce the capability of the glove. In comparison, our glove system includes a stable linkage driven structure while keeping the weight in the middle in comparison to the four other devices it was compared to. Our glove system was design to actuate all five fingers and can generate sufficient force for ADLs. The SEAs with force-based control provide the ability to grasp different objects with proper force, which can be used for the latter stages of physical therapy or intelligent control. The integration of a personalized voice activation function increases the convenience of daily use for patients.

VI. CONCLUSION AND FUTURE WORK

The proposed rehabilitation glove system has been proved to be able to restore hand functionality through a series of grasping experiments. Our research aims to remedy the shortcomings in previous strategies to create a lightweight and portable robotic hand exoskeleton. The mechanical, electrical, and software design were discussed, and grasping experiments with a normal hand were performed to test the functionality and robustness of the glove. We believe that the proposed system is innovative and comfortable to wear due to its combination of portability and dexterity, enabled by novel actuation and control methodologies developed by our team. The glove system will be tested with patients who suffer from Brachial Plexus injuries in the near future in collaboration with Dr. Cesar Bravo at the Carilion Clinic Institute of Orthopaedics and Neurosciences in Roanoke, VA. The intelligent control of the glove system based on perception of contact forces and hand posture will be implemented in future research.

REFERENCES

[1] J. L. Giuffre, S. Kakar, A. T. Bishop, R. J. Spinner, and A. Y. Shin, "Current Concepts of the Treatment of Adult Brachial Plexus Injuries," *Journal of Hand Surgery*, vol. 35, no. 4, pp. 678–688, 4 2010.

[2] P. Polygerinos, Z. Wang, K. C. Galloway, R. J. Wood, and C. J. Walsh, "Soft robotic glove for combined assistance and at-home rehabilitation," *Robotics and Autonomous Systems*, vol. 73, pp. 135–143, 2015.

[3] S. Kudo, K. Oshima, M. Arizono, Y. Hayashi, and S. Moromugi, "Electric-powered glove for CCI patients to extend their upper-extremity function," in *2014 IEEE/SICE International Symposium on System Integration, SII 2014*. Institute of Electrical and Electronics Engineers Inc., 1 2014, pp. 638–643.

[4] "Gloreha glove." https://www.gloreha.com/, accessed: 2022-02-02.

[5] C. J. Nycz, T. Bützer, O. Lambercy, J. Arata, G. S. Fischer, and R. Gassert, "Design and characterization of a lightweight and fully portable remote actuation system for use with a hand exoskeleton," *IEEE Robotics and Automation Letters*, vol. 1, no. 2, pp. 976–983, 2016.

[6] X. Hu, K. Tong, X. Wei, W. Rong, E. Susanto, and S. Ho, "The effects of post-stroke upper-limb training with an electromyography (emg)-driven hand robot," *Journal of Electromyography and Kinesiology*, vol. 23, no. 5, pp. 1065–1074, 2013.

[7] N. S. Ho, K. Y. Tong, X. L. Hu, K. L. Fung, X. J. Wei, W. Rong, and E. A. Susanto, "An EMG-driven exoskeleton hand robotic training device on chronic stroke subjects: Task training system for stroke rehabilitation," in *IEEE International Conference on Rehabilitation Robotics*, 2011.

[8] Y. Guo, W. Xu, S. Pradhan, C. Bravo, and P. Ben-Tzvi, "Personalized voice activated grasping system for a robotic exoskeleton glove," *Mechatronics*, vol. 83, p. 102745, 2022.

[9] T. Vanteddu, B. Sebastian, and P. Ben-Tzvi, "Design optimization of RML glove for improved grasp performance," in *ASME 2018 Dynamic Systems and Control Conference, DSCC 2018*, vol. 1. American Society of Mechanical Engineers (ASME), 2018.

[10] E. M. Refour, B. Sebastian, R. J. Chauhan, and P. Ben-Tzvi, "A General Purpose Robotic Hand Exoskeleton With Series Elastic Actuation," *Journal of Mechanisms and Robotics*, vol. 11, no. 6, 12 2019.

[11] R. J. Chauhan and P. Ben-Tzvi, "Latent variable grasp prediction for exoskeletal glove control," *ASME 2018 Dynamic Systems and Control Conference, DSCC 2018*, vol. 1, pp. 1–7, 2018.

[12] T. Feix, J. Romero, H. B. Schmiedmayer, A. M. Dollar, and D. Kragic, "The GRASP Taxonomy of Human Grasp Types," *IEEE Transactions on Human-Machine Systems*, vol. 46, no. 1, pp. 66–77, 2016.

[13] B. J. Lee, A. Williams, and P. Ben-Tzvi, "Intelligent Object Grasping with Sensor Fusion for Rehabilitation and Assistive Applications," *IEEE Transactions on Neural Systems and Rehabilitation Engineering*, vol. 26, no. 8, pp. 1556–1565, 2018.

[14] Y. Guo, W. Xu, S. Pradhan, C. Bravo, and P. Ben-Tzvi, "Integrated and Configurable Voice Activation and Speaker Verification System for a Robotic Exoskeleton Glove," ser. International Design Engineering Technical Conferences and Computers and Information in Engineering Conference, vol. Volume 10: 44th Mechanisms and Robotics Conference (MR), 08 2020.

[15] Y. Guo, W. Xu, S. Pradhan, C. Bravo, and P. Ben-Tzvi, "Data driven calibration and control of compact lightweight series elastic actuators for robotic exoskeleton gloves," *IEEE Sensors Journal*, 07 2021.

[16] J. B. Lee, "Development of Intelligent Exoskeleton Grasping Through Sensor Fusion and Slip Detection Development of Intelligent Exoskeleton Grasping," Master's thesis, Virginia Polytechnic Institute and State University, 2018.

[17] D. Ryu, K.-W. Moon, H. Nam, Y. Lee, C. Chun, S. Kang, and J.-B. Song, "Micro hydraulic system using slim artificial muscles for a wearable haptic glove," in *2008 IEEE/RSJ International Conference on Intelligent Robots and Systems*. IEEE, 2008, pp. 3028–3033.